



Characterizing leaf-scale fluorescence with spectral invariants

Wendi Lu^{a,b}, Yelu Zeng^{a,b,*}, Nastassia Vilfan^c, Jianxi Huang^d, Shari Van Wittenberghe^e,
Yachang He^{a,b}, Yongyuan Gao^{a,b}, Laura Verena Junker-Frohn^f, Jennifer E. Johnson^g,
Wei Su^{a,b}, Qinhuo Liu^h, Bastian Siegmann^f, Dalei Hao^{i,*}

^a College of Land Science and Technology, China Agricultural University, Beijing 100083, China

^b Key Laboratory of Remote Sensing for Agri-Hazards, Ministry of Agriculture and Rural Affairs, Beijing 100083, China

^c University of Twente, Faculty of Geo-Information Science and Earth Observation (ITC), P.O. Box 217 AE, Enschede 7500, the Netherlands

^d Faculty of Geosciences and Engineering, Southwest Jiaotong University, Chengdu 611756, China

^e Laboratory for Earth Observation (LEO), Image Processing Laboratory (IPL), Parc Científic, Universitat de València, 46980 Paterna, València, Spain

^f Institute of Bio- and Geosciences, IBG-2: Plant Sciences, Forschungszentrum Jülich GmbH, Wilhelm-Johnen-Straße, 52428 Jülich, Germany

^g Department of Ecology & Evolutionary Biology, University of Kansas, Lawrence, KS 66045, United States

^h State Key Laboratory of Remote Sensing Science, Aerospace Information Research Institute, Chinese Academy of Sciences, Beijing 100101, China

ⁱ Atmospheric, Climate, & Earth Sciences Division, Pacific Northwest National Laboratory, United States

ARTICLE INFO

Editor: Jing M. Chen

Keywords:

Sun-induced fluorescence (SIF)
Leaf scale radiative transfer
Spectral invariants theory
Photon recollision probability

ABSTRACT

Sun-induced chlorophyll fluorescence (SIF) is increasingly recognized as a non-destructive probe for tracking terrestrial photosynthesis. Emerging developments in spectral invariants theory provide an innovative and efficient approach for representing SIF radiative transfer processes at the canopy scale. However, modeling leaf-scale fluorescence based on the spectral invariants properties (SIP) remains underexplored. In this study, the spectral invariants theory is employed for the first time to model the leaf-scale total, backward and forward fluorescence (leaf-SIP SIF). The leaf-SIP SIF model separates the leaf-scale radiative transfer process into two distinct components: the wavelength-dependent one associated with leaf biochemical properties, and the wavelength-independent component linked to leaf structural characteristics. The leaf structure-related effects are characterized by two spectrally invariant parameters: the photon recollision probability (p) and the scattering asymmetry parameter (q), which are parameterized using the directly measurable leaf dry matter. Evaluation against field measurements shows that the proposed leaf-SIP SIF model has a good performance, with coefficient of determination (R^2) of 0.89, 0.89, 0.90 and root mean squared errors (RMSE) of 1.28, 0.69, 0.74 $\text{Wm}^{-2}\mu\text{m}^{-1}\text{sr}^{-1}$, respectively for the total, backward, and forward fluorescence (660–800 nm). The leaf-SIP SIF model with a more concise formulation demonstrates comparable performance with the widely used Fluspect model. The leaf-SIP SIF model provides a simple and efficient approach for simulating leaf-scale fluorescence, with the potential to be integrated into a unified SIP-based model framework for simulating the radiative transfer processes across the soil-leaf-canopy-atmosphere continuum.

1. Introduction

Sun-induced chlorophyll fluorescence (SIF) is directly linked to plant photosynthesis, and provides an efficient way of non-destructive monitoring of plant photosynthesis and the physiological status of vegetation (Krause and Weis, 1991). In recent years, SIF has been widely used in gross primary productivity monitoring (Zhang et al., 2016; Hao et al., 2021), plant stress detection (Kimm et al., 2021; Zeng et al., 2022), crop yield estimation (Guan et al., 2016), and terrestrial carbon cycle (Sun

et al., 2017). Given its important role in plant physiology and ecosystem processes, SIF has become a critical tool for remotely sensed environmental and ecological monitoring.

As the field of SIF research advances, accurately modeling leaf-scale fluorescence becomes increasingly essential for simulating fluorescence in relation to plant health, growth, and carbon dynamics. Leaf-scale fluorescence has been modelled using radiative transfer models, which can be categorized into three groups according to their original theoretical basis. The first category is the model based on Kubelka-Munk (K-

* Corresponding author at: College of Land Science and Technology, China Agricultural University, Beijing 100083, China.

E-mail addresses: zengyelu@163.com (Y. Zeng), dalei.hao@pnnl.gov (D. Hao).

<https://doi.org/10.1016/j.rse.2025.114704>

Received 14 April 2024; Received in revised form 3 March 2025; Accepted 6 March 2025

Available online 12 March 2025

0034-4257/© 2025 Elsevier Inc. All rights are reserved, including those for text and data mining, AI training, and similar technologies.

M) theory and Beer's law. Rosema et al. (1991) proposed a novel leaf-scale fluorescence model, based on the K-M theory, and Ounis et al. (2001) modelled leaf-scale fluorescence based on the Beer's law assumptions. The second category involves radiative transfer modeling, such as the FluorMODleaf (Pedrós et al., 2010) and the Fluspect (Vilfan et al., 2016). The latter was developed from the PROSPECT model (Jacquemoud and Baret, 1990). The third category involves models utilizing the Monte Carlo simulations. Sušila and Naus (2007) and Zhao and Ni (2018) used the Monte Carlo approaches to simulate the leaf-scale fluorescence.

While these models have provided valuable insights into leaf-scale fluorescence, they all have limitations that hinder their widespread application. The models based on K-M theory and Beer's law often fail to capture the complexity of light scattering and absorption in leaves, especially for complex leaf structures. The FluorMODleaf and Fluspect models offer higher accuracy in modeling leaf fluorescence but are relatively complex and computationally demanding. Monte Carlo methods, though highly accurate in simulating photon transport, are computationally expensive, with accuracy heavily dependent on the number of photons tracked.

Given these challenges, the spectral invariants theory presents a promising alternative. The spectral invariants theory has been successfully used to describe photon interactions within the vegetation canopy through the spectrally invariant parameters related to the canopy structural properties. Introduced by Knyazikhin et al. (1998), this theory provided a novel approach for modeling radiation transmission in vegetation, and has been used in various applications. For example, a semi-empirical model was developed to simulate the canopy bidirectional reflectance factor (BRF) by incorporating the upward escape probability ρ_{up} and the asymmetry factor q (Mottus and Stenberg, 2008). Additionally, the theory has been used to monitor vegetation dynamics by the Earth Polychromatic Imaging Camera (Marshak and Knyazikhin, 2017), where the retrieval of the spectrally invariant coefficient provides accurate estimates of the canopy reflectance. Majasalmi et al. (2014) proposed a model based on this theory to simulate the fraction of absorbed photosynthetically active radiation (fPAR) through the leaf area index (LAI), canopy gap fractions, and spectra of foliage and understory. Moreover, the theory has been applied to develop a practical approach for estimating the canopy-scale escape ratio of SIF (Zeng et al., 2019). Overall, these studies demonstrate the unique potential of the spectral invariants theory in characterizing canopy-scale radiative transfer processes.

Yet, the application of the spectral invariants theory to leaf scale radiative transfer modeling is just beginning to be explored. A first attempt to parameterize the single scattering albedo of a leaf based on the photon recollision probability used a function of the wavelength-dependent refractive index (Lewis and Disney, 2007). However, this method did not fully follow the spectral invariants theory because the photon recollision probability should be wavelength independent (Mottus and Stenberg, 2008; Smolander and Stenberg, 2005; Stenberg, 2007). More recently, Wu et al. (2021) developed a leaf-scale radiative transfer model based on the spectral invariants theory (leaf-SIP optical) for simulating leaf reflectance and transmittance. However, the application of the spectral invariants theory to simulate leaf-scale fluorescence remains under-explored. It is promising to further investigate the feasibility of describing leaf-level radiative transfer of fluorescence and simulating the leaf-scale fluorescence spectrum based on the spectral invariants theory.

The objective of this study is to develop a simple leaf-scale radiative transfer model based on the spectral invariants theory (leaf-SIP SIF), for simulating the total, backward and forward fluorescence in response to leaf biochemical and physical structure properties. First, we described the radiative transfer process at the leaf scale by conceptualizing the leaf interior as a composition of the basic particles for the leaf optical and fluorescence model scale. Second, we recalibrated the spectrally invariant parameters photon recollision probability p (Stenberg, 2007)

and scattering asymmetry parameter q (Mottus and Stenberg, 2008) based on the LOPEX and ANGERS datasets. Then we simulated leaf fluorescence by calculating the difference between two scenarios: the first includes the radiative transfer process of both fluorescence and scattering, while the second scenario only considers the scattering process. Third, we evaluated the leaf-SIP SIF model against field measurements, and compared its performance with the widely-used Fluspect model. Additionally, the sensitivity of the newly developed leaf-SIP SIF model was assessed under varying combinations of leaf biochemical parameters.

2. Model development

2.1. Theoretical basis of the leaf-SIP SIF model

The leaf-SIP SIF model represents the internal radiative transfer within the leaf as a stochastic process. The proposed model is based on the leaf-SIP optical model presented by Wu et al. (2021) and extends this framework with a more detailed hierarchical description of the leaf internal scattering elements (Fig. 1). To introduce our approach, we will begin by explaining how the physical hierarchy in the organization of leaves corresponds to the hierarchy of leaf internal scattering elements in our model.

In physical terms, there are many levels to the hierarchical organization of the internal structural components of leaves that are potentially relevant to modeling chlorophyll fluorescence. In particular, leaves are internally organized into epidermal, mesophyll, and vascular tissues, and the mesophyll tissue is composed of cells containing chloroplasts. Chloroplasts are further organized into the stroma, which contains the soluble enzymes mediating carbon fixation, and the thylakoid membranes, which contain the pigments and proteins mediating electron transport and ATP synthesis. The pigments and proteins are organized into pigment-protein complexes termed photosystems, within which each reaction center is grouped together in antenna complexes with many individual chlorophyll molecules (for a comprehensive review, see Porcar-Castell et al., 2021).

In the leaf-SIP SIF model, we abstract this physical hierarchy into two mathematical levels of organization which determine photon scattering within the leaf: 'small particles' which represent the pigments that are grouped together within photosystem, and 'large particles', which represent the photosystems that are embedded within the thylakoid membranes of chloroplasts (Fig. 1). The antenna complexes of Photosystem I and Photosystem II each contain hundreds of individual chlorophyll molecules, and thus they are relatively larger in size than the single pigments. These two types of particles are also regarded as the basic leaf internal scattering elements in the leaf-SIP optical model for the upscaling to the leaf level (Wu et al., 2021).

Our treatment extends that of Wu et al. (2021) by introducing fluorescence. To describe the spectral distribution of fluorescence, we use the composite photosystem-level spectrum developed by van der Tol et al. (2019) for 'large particles'. Although in physical terms fluorescence is originally generated by small particles (i.e., chlorophyll molecules), we treat the photosystem as the basic leaf internal element for the fluorescence generation calculations.

Therefore, fluorescence is generated upon the incident photons collision with photosystems as large particles within the leaf. After fluorescence generation, re-absorption and scattering occur when photons collide with other different particles within the leaf. This nested hierarchical arrangement plays a vital role in determining the size of the photosystem as a large particle, which is essential for the fluorescence generation calculation before re-absorption by other photosystems.

Furthermore, this approach allows the proposed model to capture the overall light scattering and absorption processes within the leaf while simplifying the radiative transfer computation. This hierarchical representation depicts the radiative transfer of a leaf through a series of such interactions and reflects the random nature of photon interactions

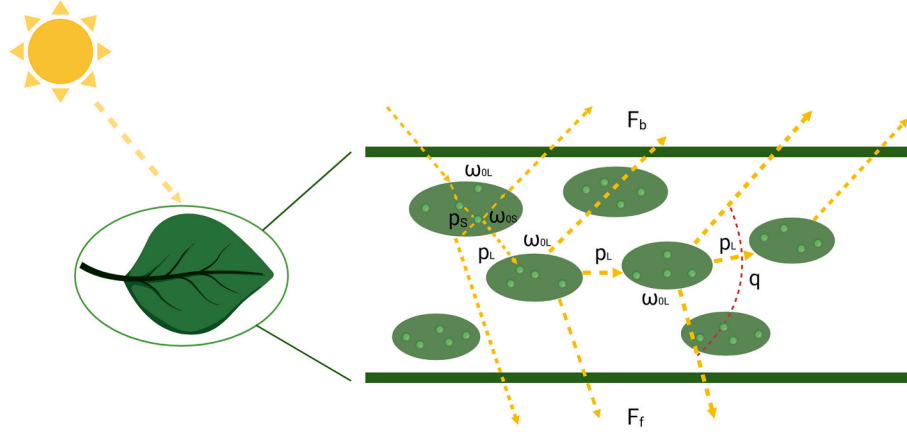


Fig. 1. Schematic diagram of the leaf-scale radiative transfer processes of fluorescence in the leaf-SIP SIF model. The small particles in this figure are represented by light green circles, corresponding to individual, isolated pigments (e.g., chlorophyll). The large particles are represented by dark green ellipses, corresponding to individual, isolated photosystems. F_b is the backward fluorescence and F_f is the forward fluorescence; ω_{0L} and ω_{0S} are the single scattering albedo of the large and small particles, respectively; p_L is the probability that a photon recollides with other small particles within another large particle after the previous collision, p_S is the probability that a photon recollides with other small particles in the same large particle after the previous collision, and q is the scattering asymmetry parameter that determines the proportion of F_b and F_f in leaf-scale fluorescence. All variables except p and q are wavelength-dependent. (For interpretation of the references to colour in this figure legend, the reader is referred to the web version of this article.)

at different spatial scales in the leaf structure. Particularly, the probability of photons re-colliding with the leaf basic scattering element (Wu et al., 2021)—whether large or small particle, is primarily influenced by the leaf structure, rather than the photon wavelength, as stated by Stenberg et al. (2016).

2.2. Spectral invariants in the leaf-SIP SIF model

In the leaf-SIP SIF model, the scattering albedo for large particles (ω_{0L}) is calculated in the same way as in the leaf-SIP optical model: as the sum of the geometric sequence of scattering from small particles. This is derived from the probability that a photon recollides with other small particles after the previous collision within the same large particle (p_S) (Lewis and Disney, 2007) and the underlying reference scattering albedo ω_{0S} .

$$\omega_{0L} = \omega_{0S} \frac{1 - p_S}{1 - p_S \omega_{0S}} \quad (1)$$

The definition of ω_{0S} follows the one described in the Fluspect model:

$$\omega_{0S} = \exp(-A_i) = \exp\left(-\sum_{i=1}^m \frac{C_i k_i(\lambda)}{\beta C_{dm}}\right) \quad (2)$$

The reference scattering albedo ω_{0S} is directly derived from the absorption spectrum A_i of the leaf biochemical constituents (Lewis and Disney, 2007; Marshak and Knyazikhin, 2017), and m is the number of leaf biochemical constituents. Each component is characterized by two main factors: C_i and $k_i(\lambda)$. C_i denotes the mass of the i th leaf biochemical constituent per unit leaf area, and $k_i(\lambda)$ is the corresponding specific absorption coefficient. The biochemical components include chlorophyll $a + b$ (C_{ab}), carotenoids (C_x), anthocyanins (C_{anth}), brown pigments (C_{brown}), water equivalent thickness (C_w), and dry matter (C_{dm}). β is a scaling constant used to adjust the concentration of these biochemical constituents from per unit leaf area to density metric, following the description in the leaf-SIP optical model (Wu et al., 2021).

In accordance with the leaf-SIP optical model (Wu et al., 2021), the probability that a photon recollides with other small particles in the same leaf after the previous collision (Stenberg et al., 2016) is a function of C_{dm} :

$$p = 1 - \frac{1 - \exp(-f(C_{dm}))}{f(C_{dm})} \quad (3)$$

where $f(C_{dm})$ was formulated in Wu et al. (2021) (Eq. 4), and calibrated using the LOPEX and ANGERS datasets.

$$f(C_{dm}) = k_1 C_{dm} \quad (4)$$

The probability that a photon recollides with other small particles within another large particle after the previous collision, p_L , is related to p , or fundamentally, leaf thickness (Stenberg et al., 2016). To maintain that p_L remains within a reasonable range and ensure calculation stability, we utilized a least-square approach to iteratively adjust parameters and minimize the error between the leaf-SIP SIF model-simulated upward and downward fluorescence and the measured results. The range of p_L was set as the minimum value of 0.9 ($C_{dm} = 0.004$) and p :

$$p_L = \min(p, 0.9) \quad (5)$$

Then p_S , the probability that a photon recollides with other small particles in the same large particle after the previous collision, can be derived as a function of p and p_L (Smolander and Stenberg, 2005):

$$p_S = \frac{p - p_L}{1 - p_L} \quad (6)$$

When fluorescence is generated from photosystems within the leaf, it can escape from the leaf either in the forward or backward direction. The upward escape probability ρ_n^{up} of a photon depends on the scattering order n and can be described as (Mottus and Stenberg, 2008; Wu et al., 2021):

$$\rho_n^{up} = \frac{(1 - p_L)(1 + q^n)}{2} \quad (7)$$

In contrast to the q in the leaf-SIP optical model, the q in Eq. (7) is always positive and ranges from 0 to 1. In the leaf optical model, q could be positive when the leaf is thick and the leaf reflectance is higher than the transmittance, and could be negative when the leaf is thin and the leaf reflectance is lower than the transmittance. However, in the leaf-SIP SIF model, q is always positive, which means that F_b is always higher than F_f . This is because within the leaf, fluorescence photons are only emitted when the photosystems within the leaf intercept incident solar photons. Furthermore, due to the strong absorption and scattering effects of the fluorescence inside the leaf, and a higher chlorophyll content around the adaxial epidermis, there is an obvious difference in fluorescence radiance between the adaxial and abaxial sides of the leaf (Jia et al., 2018). The exact fitting procedure for q can be found in Section

3.2.

2.3. Leaf-scale fluorescence calculations

The calculation of leaf-scale fluorescence follows a three-step approach that Zeng et al. (2020) introduced for calculation of canopy fluorescence based on the spectrally invariant parameters. First, the radiative transfer process is calculated including both fluorescence and scattering; second, the calculations are repeated for scattering alone; and third, the differences between the two calculations are used to isolate fluorescence. We assume that a photon is scattered n times by large particles before leaving the leaf, and the leaf-scale fluorescence can be calculated as the sum of the n orders scattering. As assumed by Stenberg et al. (2016), the irradiance corresponding to an $(n + 1)$ -th order collision $Q_{n+1}^\sigma(\lambda_f)$ can be derived from the irradiance of the n -th order colliding photon in the horizontal plane $Q_n^\sigma(\lambda_f)$ combined with the recollision probability via a recursive sequence:

$$Q_{n+1}^\sigma(\lambda) = \begin{cases} Q_{dir}(\lambda, \Omega_0) \cdot i_0(\Omega_0), n = 0 \\ Q_n^\sigma(\lambda) \cdot \omega_{0L}(\lambda) \cdot p_L + \int_{400}^{750} Q_n^\sigma(\lambda_e) \cdot M_n(\lambda_e, \lambda_f) \cdot p_L d\lambda_e, n \geq 1 \end{cases} \quad (8)$$

where σ is the superscript of Q denoting photon extinction or collision, Q_{dir} is the direct light irradiance over the horizontal surface at wavelength λ , coming from direction Ω_0 , and i_0 is the probability of interception, assumed to be 1 in the leaf SIP SIF model. If $n \geq 1$, $Q_{n+1}^\sigma(\lambda)$ is a function of the intercepted irradiance at wavelength λ , termed $Q_n^\sigma(\lambda)$, and the intercepted irradiance at wavelength λ_e , termed $Q_n^\sigma(\lambda_e)$. $M_n(\lambda_e, \lambda_f)$ is the leaf fluorescence excitation-emission matrix, where the first index denotes the excitation wavelengths λ_e from 400 to 750 nm and the second index denotes the emission wavelengths λ_f from 640 to 850 nm (van der Tol et al., 2009). The Fluspect model assumes that the interior of the leaf consists of m layers and calculates the fluorescence excitation-emission matrix of the mesophyll layer by the doubling algorithm (van der Tol et al., 2009). In contrast, we added S_{ab} to calculate the leaf fluorescence excitation-emission matrix at the large particle level:

$$M_n(\lambda_e, \lambda_f) = 0.5S_{ab}\Phi_F\phi(\lambda_f)k_{chl}(\lambda_e)\sigma(\lambda_e, \lambda_f) \quad (9)$$

$$S_{ab} = k_2C_{ab} + C_1 \quad (10)$$

where S_{ab} is the correction coefficient, and we fitted its specific form in Eq. (10) by a least-square approach. Φ_F represents the fraction of absorbed energy emitted as fluorescence, and $\phi(\lambda_f)$ is the probability density function describing the likelihood that a fluorescence photon has a specific wavelength λ_f . It is important to note that both of these are composite parameters that are influenced by the properties of Photosystem II as well as Photosystem I (i.e., including their individual absorption cross-sections, as well as fluorescence spectra). $k_{chl}(\lambda_e)$ is the Kubelka-Munk absorption coefficient for chlorophyll, $\sigma(\lambda_e, \lambda_f)$ is a matrix that reduces anti-Stokes fluorescence at shorter wavelengths than the excitation light in the model, and the $\phi(\lambda_f)$, $k_{chl}(\lambda_e)$, and $\sigma(\lambda_e, \lambda_f)$ are consistent with those specified of the layers at the photosystem level in the Fluspect model (van der Tol et al., 2009). After calibrating, $k_2 = 0.0026$ and $C_1 = 0.38$.

The leaf reference albedo at wavelength λ_f , $\omega_{0L}(\lambda_f)$, and p_L have the same values in different scattering orders. The total and backward leaving irradiance from the n -th order collision, including the scattered radiation and generated fluorescence in the horizontal plane are

$$Q_n^{tot} = Q_n^\sigma(\lambda)\omega_{0L}(\lambda)\rho_n^{tot} + \int_{400}^{750} Q_n^\sigma(\lambda_e)M_n(\lambda_e, \lambda_f)\rho_n^{tot}d\lambda_e \quad (11)$$

$$Q_n^{up} = Q_n^\sigma(\lambda)\omega_{0L}(\lambda)\rho_n^{up} + \int_{400}^{750} Q_n^\sigma(\lambda_e)M_n(\lambda_e, \lambda_f)\rho_n^{up}d\lambda_e \quad (12)$$

where ρ_n^{tot} is the photon recollision probability at the n -th order collision, expressed as $1-p_L$, whose value does not change in different orders.

Similarly, we can obtain the total and backward leaving irradiance of the leaf without considering the fluorescence. Initially, the irradiance in the case of considering only the scattering is subtracted from the sum of the irradiance of the scattered radiation on the horizontal plane with the fluorescence. Then, the sum of the integrals from different orders is combined to obtain the total irradiance of the fluorescence generated by the leaf.

$$F_{tot} = \sum_{n=1}^{\infty} \int_{400}^{750} Q_n^\sigma(\lambda_e)M_n(\lambda_e, \lambda_f)\rho_n^{tot}d\lambda_e \quad (13)$$

$$F_b = \sum_{n=1}^{\infty} \int_{400}^{750} Q_n^\sigma(\lambda_e)M_n(\lambda_e, \lambda_f)\rho_n^{up}d\lambda_e \quad (14)$$

$$F_f = F_{tot} - F_b \quad (15)$$

where F_{tot} is total leaf fluorescence on two sides (the sum of backward fluorescence and forward fluorescence), F_b is backward fluorescence, and F_f is forward fluorescence.

3. Materials and methods

3.1. Datasets

We used the publicly available LOPEX and ANGERS leaf optical datasets (Feret et al., 2008), which are widely used in the model evaluation (Wu et al., 2021; Ma and Fang, 2023). The fluorescence data used in this study is a well-established and publicly accessible dataset provided by van der Tol et al. (2019), which was measured in a greenhouse located at Campus Klein Altendorf, approximately 100 km from Aachen. The dataset includes measured reflectance, transmittance and fluorescence of 66 healthy leaves from two soybean varieties, which covered a wide range of leaf chlorophyll content. Leaf scale measurements of reflectance, transmittance and fluorescence were performed with a spectro-radiometer (FieldSpec 4, Malvern Panalytical Ltd.) in combination with FluoWat leaf clip (Alonso et al., 2007). The FluoWat is a portable device to measure leaf backward and forward fluorescence. The clip has a 45° light entrance and a short-pass filter that blocks the passage of light above 650 nm during the measurement, as well as two vertical fiber optic openings, located at the top and bottom of the clip. Each measurement was repeated five times and averaged to reduce the random errors.

3.2. Modeling the spectral invariant property q

As outlined in Section 2, the two important spectrally invariant parameters in the calculation of leaf-scale fluorescence are the recollision probability p and the scattering asymmetry parameter q . We calibrated the relationship between C_{dm} and q using the LOPEX and ANGERS datasets. This involved enumerating all leaf parameters and reducing the differences between F_b and F_f as predicted by the leaf-SIP SIF and Fluspect models, respectively. The calibration was achieved by the least-squares approach under varying leaf parameters. We sampled q values from 0 to 1 in an increment of 0.01 and iterated different forms of function to determine the best q for different C_{dm} values. The relationship between C_{dm} and the estimated q value is illustrated in Fig. 2.

Finally, we can obtain the relationship between q and C_{dm} as:

$$q = \frac{1}{g(C_{dm})} + C_2 \quad (16)$$

where $g(C_{dm})$ is a monotonically decreasing function of C_{dm} , which is fitted as $g(C_{dm}) = 0.817 + \frac{0.00094}{C_{dm}}$, and $C_2 = -0.4437$.

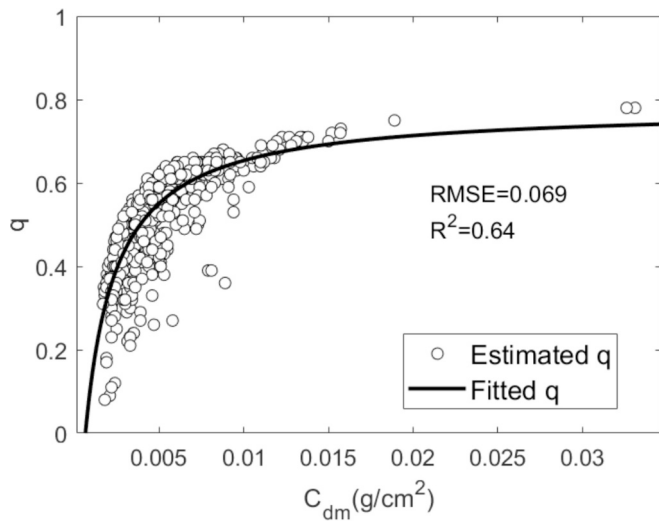


Fig. 2. Relationship between q and C_{dm} , derived from the LOPEX and ANGERS datasets.

3.3. Evaluating the leaf-SIP SIF model

First, we obtained the input leaf biochemical parameters of our newly developed leaf-SIP SIF model and Fluspect model through the model inversion. In the work of van der Tol et al. (2019), the leaf biochemical parameters were retrieved using the reflectance and transmittance simulation components of the Fluspect model. Similarly, the leaf-SIP optical model was used to retrieve leaf biochemical parameters to drive the leaf-SIP SIF model. As the leaf-SIP optical model does not involve the leaf structural parameter N , a linear relationship between N and the C_{dm} data from the LOPEX and ANGERS datasets was

developed (Wu et al., 2021). We then used C_{dm} to describe N in the forward simulations. The Fluspect model also used the leaf biochemical parameters retrieved from the measured reflectance and transmittance by the Fluspect model as inputs for simulating leaf fluorescence. Additionally, Φ_F is derived using an inversion model similar to the approach utilized in the work of van der Tol et al. (2019).

Next, we simulated leaf-scale fluorescence by inputting the biochemical parameters and incident irradiance of the leaf from the previous inversion, as described in Eqs. (13)–(15). Then we compared the simulated results of leaf fluorescence between the leaf-SIP SIF model and the Fluspect model. We used the coefficient of determination (R^2), root mean square error (RMSE) and the index of agreement (d) as metrics to evaluate each model with experimental spectroscopy measurements. The descriptive statistic d quantifies the level of consistency between the simulation results of two models (Willmott, 1981). A value of d close to 1 represents a better model agreement, while a value close to 0 shows the lack of agreement between the models.

Furthermore, to analyze the sensitivity of the leaf-SIP SIF model to different leaf biochemical parameters, we used the one-by-one local sensitivity analysis to quantify the impacts of different parameter contents on the F_{tot} , F_b and F_f .

4. Results

4.1. Performance of the leaf-SIP SIF model

We compared the total, backward and forward fluorescence simulated by the leaf-SIP SIF model with the Fluspect model, and validated the model simulations against the field measurements. The simulated and measured F_{tot} , F_b and F_f for five representative leaves are presented in Fig. 3. Then, the comparisons between simulated and measured fluorescence at the double-peak positions of fluorescence (685 nm and 745 nm) for 66 leaves are shown in Fig. 4, with summary statistics in

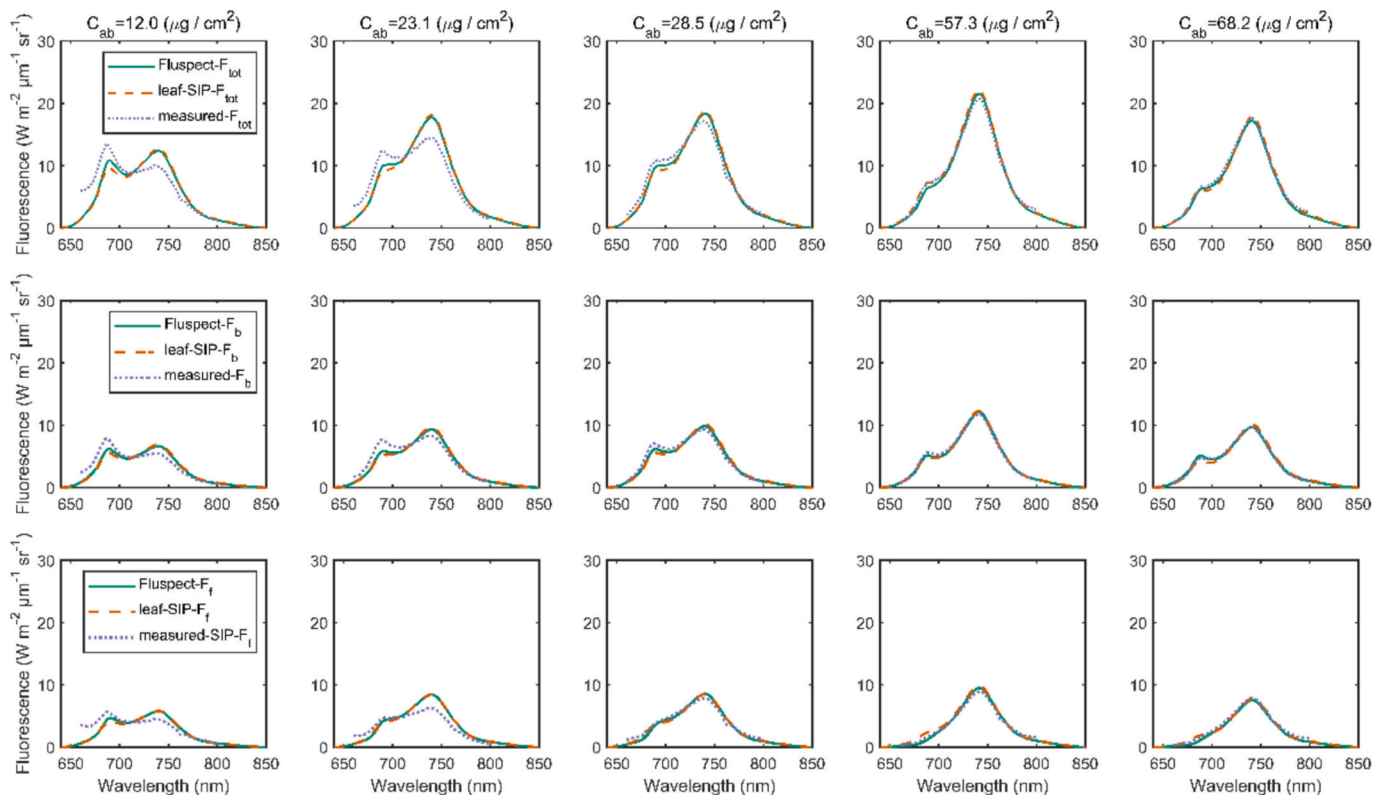


Fig. 3. Comparison of the total fluorescence F_{tot} (top), backward fluorescence F_b (second row) and forward fluorescence F_f (bottom row) between simulations from the leaf-SIP SIF model and Fluspect and field measurements. The columns correspond to varying chlorophyll concentrations (C_{ab}) ranging from 12.0 to 68.2 $\mu\text{g}/\text{cm}^2$.

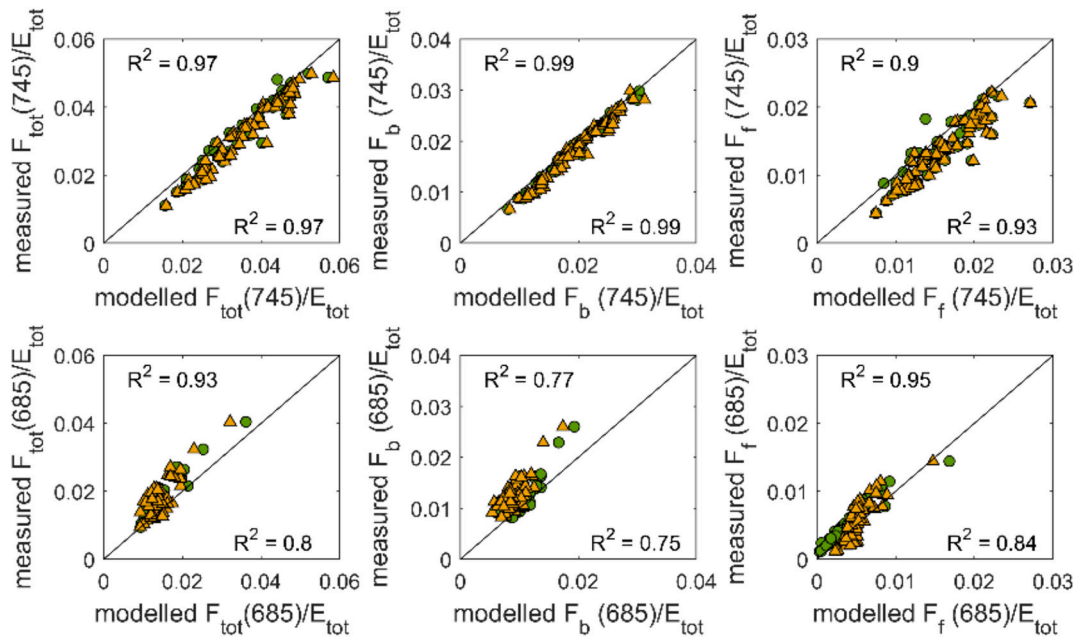


Fig. 4. Comparison between measured and modelled F_{tot} , F_b and F_f for 66 soybean leaves by Fluspect (green circle) and leaf-SIP SIF (yellow triangle) models. (For interpretation of the references to colour in this figure legend, the reader is referred to the web version of this article.)

Table 1

The R^2 between measured and modelled F_{tot} , F_b and F_f for 66 soybean leaves from the leaf-SIP SIF and Fluspect models.

Fluorescence	R^2			
	leaf-SIP SIF (745 nm)	Fluspect (745 nm)	leaf-SIP SIF (685 nm)	Fluspect (685 nm)
F_{tot}	0.94	0.94	0.64	0.86
F_b	0.97	0.98	0.56	0.6
F_f	0.87	0.82	0.7	0.9

Table 1. Overall, both the leaf-SIP SIF model and the Fluspect model exhibit high accuracy in simulating leaf-scale fluorescence, with R^2 values exceeding 0.9 for F_{tot} and F_b at both 745 nm and 685 nm. Specifically, the R^2 of F_{tot} and F_b for leaf-SIP SIF model are 0.94 and 0.97 at 745 nm. The simulated fluorescence from the leaf-SIP SIF model is generally consistent with that from the Fluspect model. These results indicate a good performance of the leaf-SIP SIF model, particularly in

the near-infrared band, underscoring its reliability in simulating leaf-scale fluorescence.

The statistical distribution of the RMSE and the R^2 over the full wavelength range (660–800 nm) is shown in Fig. 5. Due to the limitations in the measurement instruments, only fluorescence in the 660–800 nm is compared, but the models can simulate leaf fluorescence across 640–850 nm. In the range of 660 to 800 nm, the leaf-SIP SIF model achieves R^2 values of 0.89, 0.89, and 0.90 for F_{tot} , F_b , and F_f , respectively. In comparison, the Fluspect model has slightly higher R^2 values of 0.92, 0.93, and 0.91. The RMSEs for the leaf-SIP SIF model are 1.28, 0.69, and 0.74 for $Wm^{-2}\mu m^{-1}sr^{-1}$ F_{tot} , F_b , and F_f , respectively, while the Fluspect model shows RMSE values of 1.10, 0.50, and 0.70 $Wm^{-2}\mu m^{-1}sr^{-1}$ for the corresponding metrics. Detailed ranges of R^2 and RMSE are listed in Table A1. In the range of 660 to 800 nm, there was a very high level of consistency between models, with d values of 0.99, 0.99, and 0.98, respectively for F_{tot} , F_b and F_f .

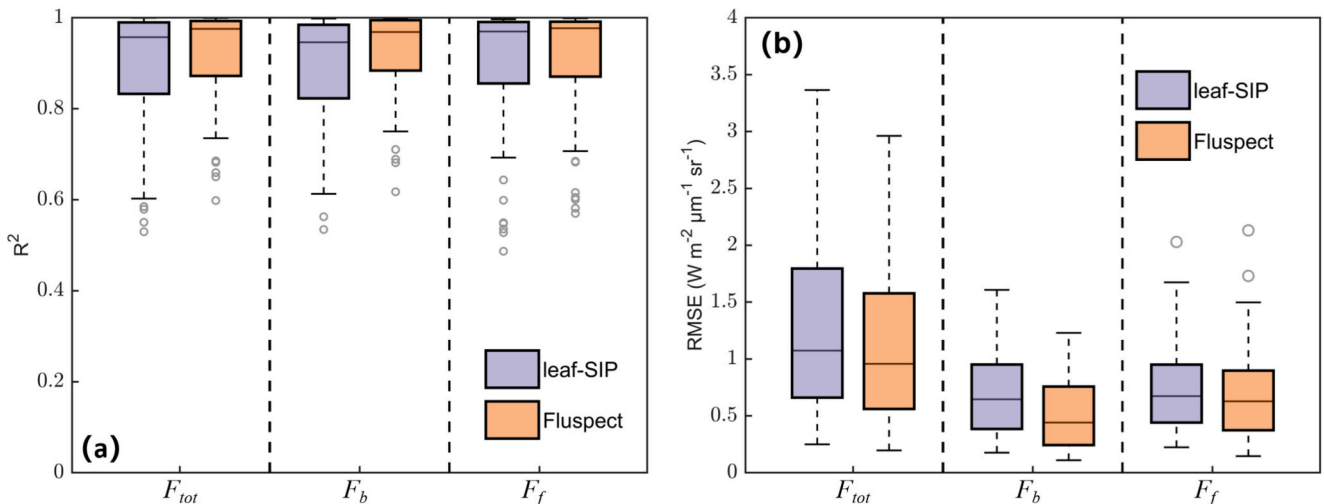


Fig. 5. Model accuracy of the leaf-SIP SIF and Fluspect models against field measurements across the 66 soybean leaves: (a) R^2 and (b) RMSE.

4.2. Sensitivity of leaf-SIP SIF model to different pigment contents

We further analyzed the fluorescence changes at either side of the leaf under different pigment contents (Fig. 6 and Table A2). As in Fig. 6 (a1-c1), the relative maximum difference (rMD, calculated as the ratio of the maximum fluorescence difference caused by the change of pigment content to the fluorescence values under the minimum pigment content) for F_{tot} in the full wavelength range reaches 36.4 %, while the F_f and F_b rMDs are 38.9 % and 37.7 %, respectively. In the near-infrared band (745 nm), the rMDs of F_{tot} , F_f and F_b are 54.3 %, 60.0 %, and 47.4 %, respectively, showing that with the increase in C_{ab} , leaf fluorescence markedly increases. However, in the red band (685 nm), the rMDs of F_{tot} , F_f and F_b are 11.2 %, 6.1 %, and 34.2 %, respectively. With the increase of C_{ab} , leaf fluorescence slightly decreases.

As in Fig. 6 (a2-c2), the influence of C_x on leaf-scale fluorescence is not as notable as that of C_{ab} . The F_{tot} rMD in the full wavelength range is 18.3 %, with the F_f and F_b rMDs being 18.5 % and 18.2 %, respectively. In the near-infrared band, the rMDs of F_{tot} , F_f and F_b are 18.3 %, 18.4 %, and 18.2 %, respectively, while they are 18.3 %, 19.0 %, and 18.1 %, respectively in the red band. Overall, leaf-scale fluorescence decreases slightly with increasing C_x , and there is little difference in the magnitude of change between F_f and F_b in the red and near-infrared bands.

The fluorescence variation under different C_{anth} levels is similar to that under different C_x values, and fluorescence shows a gradual decrease as C_{anth} increases. As depicted in Fig. 6 (a3-c3), the F_{tot} rMD in the full wavelength range reaches 11.5 %, while the F_f and F_b rMDs are 12.2 % and 11.0 %, respectively. In the near-infrared band, the rMDs of F_{tot} , F_f and F_b are 11.5 %, 12.0 %, and 11.1 %, respectively. In the red band, the rMDs of F_{tot} , F_f and F_b are 11.6 %, 13.9 %, and 10.6 %, respectively.

C_{brown} also has a notable impact on leaf-scale fluorescence. As C_{brown} increases, leaf fluorescence gradually decreases, and the magnitude of this change is more pronounced than that induced by increase of C_x and C_{anth} . As illustrated in Fig. 6 (a4-c4), the F_{tot} rMD in the full wavelength range reaches 32.7 %, while the F_f and F_b rMDs are 35.6 % and 30.6 %, respectively. In the near-infrared band, the rMDs of F_{tot} , F_f and F_b are 36.2 %, 39.0 %, and 34.3 %, respectively. In the red band, the rMDs of F_{tot} , F_f and F_b are 20.9 %, 24.1 %, and 20.0 %, respectively.

5. Discussion

5.1. Strengths of spectral invariants in leaf-scale fluorescence modeling

The potential of using SIF as a probe for nondestructive detection of vegetative photosynthesis has inspired the development of mechanistic and forward models for SIF (Grace et al., 2007; Meroni et al., 2010). In recent years, the spectral invariants theory has been applied in modeling optical reflectance at both the canopy (Zeng et al., 2020) and leaf (Wu et al., 2021) scales. In this study, we have built on these developments and extended the application of spectral invariants theory to modeling fluorescence at the leaf scale. Specifically, we have refined the description of internal leaf structure using the concept of particles, and summarized the radiative transfer process at the leaf scale using two spectrally invariant parameters (p and q). Unlike the traditional leaf-scale SIF model, the leaf-SIP SIF model eliminates the immeasurable parameter N for describing leaf structure. Instead, it utilizes the functional parameters p and q , which can be calibrated directly from measurements of leaf-scale C_{dm} . The Fluspect model employs over 100 equations to describe the radiative transfer process at the leaf scale (Vilfan et al., 2016). In contrast, the leaf-SIP SIF model simplifies the

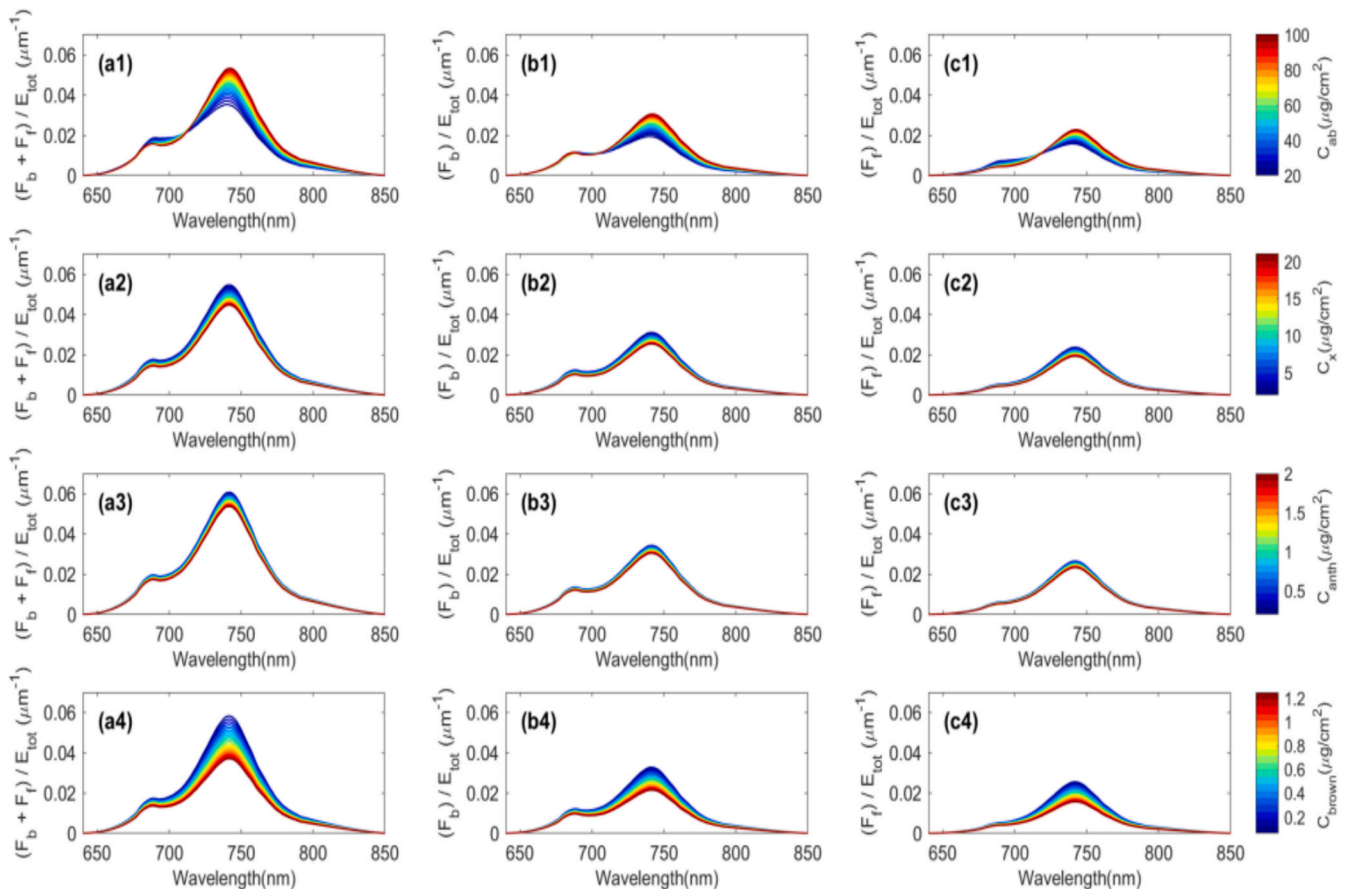


Fig. 6. Fluorescence variations under different pigment contents simulated by leaf-SIP SIF model. C_{ab} is equally spaced from 20 to 100 $\mu\text{g}/\text{cm}^2$, C_x is equally spaced from 2 to 21 $\mu\text{g}/\text{cm}^2$, C_{anth} is equally spaced from 0.2 to 4 $\mu\text{g}/\text{cm}^2$, and C_{brown} is equally spaced from 0.0625 to 1.25 $\mu\text{g}/\text{cm}^2$.

radiative transfer process and requires only 16 equations. We compared the performance in simulating leaf fluorescence between the leaf-SIP SIF and the widely-used Fluspect model. The results show that the two models have similar performance in simulating fluorescence at the leaf scale. Since the leaf-SIP SIF model achieves similar accuracy to Fluspect with much less complexity, it is a promising approach for analyzing and predicting leaf-level fluorescence.

5.2. Limitations of the current leaf-scale implementation of spectral invariants

While the leaf-SIP SIF model shows a good performance, there are a few limitations deserving further investigation. First, the spectrally invariant parameters p and q are indirect parameters related to C_{dm} . Therefore, the reliability of measured and estimated C_{dm} plays an important role in the model simulations. Second, the accuracy of the leaf-SIP SIF model in the red band decreases as chlorophyll content decreases (Fig. 3). This effect is not fully understood, but is partly due to the reduced accuracy of the inversion model when the C_{ab} is low (van der Tol et al., 2019; Wu et al., 2021). Third, there are a few uncertainties in the field-based leaf-scale fluorescence measurements. FluoWat can only measure in one direction (typically under a 25° field-of-view angle depending on the fiber optic), while an integrating sphere might be more suitable for more precise fluorescence measurements for model evaluation.

5.3. Future directions for model development and applications

We envision three key directions for development and application of this approach: (i) further refinement of the description of the leaf scattering structure within the leaf-SIP SIF model; (ii) coupling of the leaf-SIP SIF model to leaf-scale photosynthesis models that can capture the dynamic features of reflectance and fluorescence; and (iii) integration of the leaf-SIP SIF model into a larger-scale radiative transfer model that brings the spectrally invariant approach the complete leaf-canopy-atmosphere system. Each of these directions is outlined in more detail below.

In the future, one important direction is exploring whether the structure of the leaf-SIP SIF model should be revised to accommodate the heterogeneous distribution of chloroplasts within the leaf. In the study of Kallel (2020), the internal structure of the leaf was divided into two layers: palisade parenchyma and spongy mesophyll cells. In the future, we could consider constructing the leaf SIF model in two layers according to this bilayer structure. The spectral invariant parameters in the lower layer (spongy mesophyll) would still be calculated as presented in this study, while the calculation of the spectral invariant parameters p and q in the palisade parenchyma region would require further discussion. This could potentially enhance the accuracy of the leaf-SIP SIF model, especially under conditions with high chlorophyll content.

A second important direction is coupling the leaf-SIP SIF model to leaf-scale photosynthesis models that can capture the dynamic features of absorption, reflectance, and fluorescence. There are a number of fast physiological processes that have dynamic impacts on the intensity and spectral distribution of leaf absorption, reflectance, and fluorescence, such as the non-photochemical quenching mechanisms (Rajewicz et al., 2023). While these processes are not accounted for in the current leaf-SIP SIF model, they can be accounted for by coupling the leaf-SIP SIF model to a leaf-scale photosynthesis model. In general, this involves: (i) passing absorbed photosynthetically active radiation from the radiative transfer model to the photosynthesis model; (ii) calculating the state of the photosynthetic system in response to that radiation as well as other environmental properties such as temperature, humidity, and carbon dioxide; and then (iii) passing back to the radiative transfer model any relevant dynamic states that will impact absorption, reflectance, and fluorescence. Current evidence indicates that there are several processes

that can have large effects: 'qM', 'qT', 'qE', and 'qZ' (see Demmig-Adams et al., 2014 for background on this terminology). The first is the movement of chloroplasts within the leaf, which dynamically changes the total amount of photosynthetically active radiation that is absorbed versus scattered ('qM'). The second is the movement of chlorophyll pigments between the antennae of Photosystem II versus Photosystem I, which dynamically changes the spectral distribution of fluorescence ('qT'). The third is the state of the carotenoid pigments that are involved in heat-dissipating forms of non-photochemical quenching, which dynamically changes the spectral distributions of reflectance as well as fluorescence ('qE' and 'qZ'). At present, the only leaf-level photosynthesis models that both resolve all three of these processes and are efficiently invertible are those recently developed by Johnson and Berry (2021) for C_3 photosynthesis and by Johnson et al. (2021) for C_4 photosynthesis. As such, coupling these photosynthesis models to the leaf-SIP SIF model is a promising approach for capturing the features of absorption, reflection, and fluorescence that are dynamic on fast physiological timescales.

Finally, we have focused on demonstrating that the leaf-SIP SIF model is an effective tool for simulating leaf-scale fluorescence, as this opens the path to applications of this framework within much larger-scale inversions and simulations. In particular, spectral invariants theory shows promise in quantifying radiative transfer in vegetation canopy (Zeng et al., 2018) and atmosphere layer (Marshak et al., 2011). Further research could focus on developing a harmonized SIP-based leaf-canopy-atmosphere radiative transfer model, which could be promising to improve the retrievals of vegetation parameters with emerging satellite hyperspectral observations.

6. Conclusions

In this study, the spectral invariants theory was applied for the first time to describe the radiative transfer process of fluorescence at the leaf scale. We demonstrated that the recollision probability p and the scattering asymmetry parameter q can be calibrated using leaf dry matter C_{dm} . With this approach, we then compared the performance of the leaf-SIP SIF model and the Fluspect model against publicly accessible datasets. The leaf-SIP SIF model achieved R^2 values of 0.89, 0.89, 0.90 and RMSE values of 1.28, 0.69, 0.74 $Wm^{-2}\mu m^{-1}sr^{-1}$, respectively for total, backward, and forward fluorescence, while the indices of agreement of the two models were 0.99, 0.99, and 0.98. The leaf-SIP SIF model simplifies the description of the radiative transfer process, while maintaining the accuracy of the simulation of leaf-scale fluorescence. This model advances the application of the spectral invariants theory in leaf-scale fluorescence radiative transfer modeling.

CRedit authorship contribution statement

Wendi Lu: Writing – review & editing, Writing – original draft, Methodology. **Yelu Zeng:** Writing – review & editing, Writing – original draft, Methodology, Conceptualization. **Nastassia Vilfan:** Writing – review & editing, Data curation. **Jianxi Huang:** Investigation. **Shari Van Wittenberghe:** Writing – review & editing, Data curation. **Yachang He:** Methodology. **Yongyuan Gao:** Investigation. **Laura Verena Junker-Frohn:** Writing – review & editing, Data curation. **Jennifer E. Johnson:** Writing – review & editing. **Wei Su:** Investigation. **Qinhua Liu:** Investigation. **Bastian Siegmann:** Writing – review & editing, Data curation. **Dalei Hao:** Writing – review & editing, Writing – original draft, Methodology.

Declaration of competing interest

The authors declare that they do not have any commercial or associative interests that represent a conflict of interest for this work.

Data availability

The fluorescence data used in this study is a publicly accessible dataset provided by van der Tol et al. (2019).

Appendix A. Appendix

Table A1

Accuracy evaluation of the leaf-SIP SIF model against field measurements.

Model	Fluorescence	R^2	RMSE ($\text{Wm}^{-2}\mu\text{m}^{-1}\text{sr}^{-1}$)
leaf-SIP SIF	F_{tot}	0.53–1.00	0.25–3.36
leaf-SIP SIF	F_b	0.53–1.00	0.77–1.61
leaf-SIP SIF	F_f	0.49–1.00	0.22–2.03
Fluspect	F_{tot}	0.60–1.00	0.20–2.96
Fluspect	F_b	0.62–1.00	0.11–1.23
Fluspect	F_f	0.57–1.00	0.15–2.13

Table A2

Relative maximum differences (rMDs) of F_{tot} , F_b , F_f across different spectral bands during sensitivity analysis for varying leaf pigment contents.

Pigment content	Fluorescence	rMD (%) (640–850 nm)	rMD (%) (745 nm)	rMD (%) (685 nm)
C_{ab}	F_{tot}	36.4	54.3	11.2
C_{ab}	F_b	38.9	6.1	6.1
C_{ab}	F_f	37.7	47.4	34.2
C_x	F_{tot}	18.3	18.3	18.3
C_x	F_b	18.2	18.2	18.1
C_x	F_f	18.5	18.4	19.0
C_{anth}	F_{tot}	11.5	11.5	11.6
C_{anth}	F_b	11.0	11.1	10.6
C_{anth}	F_f	12.2	12	13.9
C_{brown}	F_{tot}	32.7	36.2	20.9
C_{brown}	F_b	30.6	34.3	20.0
C_{brown}	F_f	35.6	39.0	24.1

References

- Alonso, L., Gómez-Chova, L., Vila-Francés, J., Amorós-López, J., Guanter, L., Calpe, J., Moreno, J., 2007. Sensitivity Analysis of the Fraunhofer Line Discrimination Method for the Measurement of Chlorophyll Fluorescence using a Field Spectroradiometer. *IGARSS*. <https://doi.org/10.1109/IGARSS.2007.4423660>.
- Demmig-Adams, B., Garab, G., Adams III, W., Govindjee, 2014. Non-Photochemical Quenching and Energy Dissipation in Plants, Algae and Cyanobacteria, Vol. 40. Springer. <https://doi.org/10.1007/978-94-017-9032-1>.
- Feret, J.-B., François, C., Asner, G.P., Gitelson, A.A., Martin, R.E., Bidet, L.P.R., Ustin, S. L., le Maire, G., Jacquemoud, S., 2008. PROSPECT-4 and 5: advances in the leaf optical properties model separating photosynthetic pigments. *Remote Sens. Environ.* 112, 3030–3043. <https://doi.org/10.1016/j.rse.2008.02.012>.
- Grace, J., Nichol, C., Disney, M., Lewis, P., Quaife, T., Bowyer, P., 2007. Can we measure terrestrial photosynthesis from space directly, using spectral reflectance and fluorescence? *Glob. Chang. Biol.* 13, 1484–1497. <https://doi.org/10.1111/j.1365-2486.2007.01352.x>.
- Guan, K., Berry, J.A., Zhang, Y., Joiner, J., Guanter, L., Badgley, G., Lobell, D.B., 2016. Improving the monitoring of crop productivity using spaceborne solar-induced fluorescence. *Glob. Chang. Biol.* 22, 716–726. <https://doi.org/10.1111/gcb.13136>.
- Hao, D., Asrar, G.R., Zeng, Y., Yang, X., Li, X., Xiao, J., Guan, K., Wen, J., Xiao, Q., Berry, J.A., Chen, M., 2021. Potential of hotspot solar-induced chlorophyll fluorescence for better tracking terrestrial photosynthesis. *Glob. Chang. Biol.* 27, 2144–2158. <https://doi.org/10.1111/gcb.15554>.
- Jacquemoud, S., Baret, F., 1990. PROSPECT: a model of leaf optical properties spectra. *Remote Sens. Environ.* 34, 75–91. [https://doi.org/10.1016/0034-4257\(90\)90100-Z](https://doi.org/10.1016/0034-4257(90)90100-Z).
- Jia, M., Zhu, J., Ma, C., Alonso, L., Li, D., Cheng, T., Tian, Y., Zhu, Y., Yao, X., Cao, W., 2018. Difference and potential of the upward and downward sun-induced chlorophyll fluorescence on detecting leaf nitrogen concentration in wheat. *Remote Sens.* 10. <https://doi.org/10.3390/RS10081315>.
- Johnson, J.E., Berry, J.A., 2021. The role of cytochrome b6f in the control of steady-state photosynthesis: a conceptual and quantitative model. *Photosynth. Res.* 148, 101–136. <https://doi.org/10.1007/s11120-021-00840-4>.
- Johnson, J.E., Field, C.B., Berry, J.A., 2021. The limiting factors and regulatory processes that control the environmental responses of C3, C3–C4 intermediate, and C4 photosynthesis. *Oecologia* 197, 841–866. <https://doi.org/10.1007/s00442-021-05062-y>.
- Kallel, A., 2020. FluLCVRT: reflectance and fluorescence of leaf and canopy modeling based on Monte Carlo vector radiative transfer simulation. *J. Quant. Spectrosc. Radiat. Transf.* 253. <https://doi.org/10.1016/j.jqsrt.2020.107183>.
- Kimm, H., Guan, K., Burroughs, C.H., Peng, B., Ainsworth, E.A., Bernacchi, C.J., Moore, C.E., Kumagai, E., Yang, X., Berry, J.A., Wu, G., 2021. Quantifying high-temperature stress on soybean canopy photosynthesis: the unique role of sun-induced chlorophyll fluorescence. *Glob. Chang. Biol.* 27, 2403–2415. <https://doi.org/10.1111/gcb.15603>.
- Knyazikhin, Y., Martonchik, J.V., Myneni, R.B., Diner, D.J., Running, S.W., 1998. Synergistic algorithm for estimating vegetation canopy leaf area index and fraction of absorbed photosynthetically active radiation from MODIS and MISR data. *J. Geophys. Res. Atmos.* 103, 32257–32275. <https://doi.org/10.1029/98JD02462>.
- Krause, G.H., Weis, E., 1991. Chlorophyll fluorescence and photosynthesis: the basics. *Annu. Rev. Plant Physiol. Plant Mol. Biol.* 42, 313–349. <https://doi.org/10.1146/annurev.pp.42.060191.001525>.
- Lewis, P., Disney, M., 2007. Spectral invariants and scattering across multiple scales from within-leaf to canopy. *Remote Sens. Environ.* 109, 196–206. <https://doi.org/10.1016/j.rse.2006.12.015>.
- Ma, T., Fang, H., 2023. GSV-L: a general spectral vector model for hyperspectral leaf spectra simulation. *Int. J. Appl. Earth Obs. Geoinf.* 117. <https://doi.org/10.1016/j.jag.2023.103216>.

- Majasalmi, T., Rautiainen, M., Stenberg, P., 2014. Modeled and measured fPAR in a boreal forest: Validation and application of a new model. *Agric. For. Meteorol.* 189–190, 118–124. <https://doi.org/10.1016/j.agrformet.2014.01.015>.
- Marshak, A., Knyazikhin, Y., 2017. The spectral invariant approximation within canopy radiative transfer to support the use of the EPIC/DSCOVR oxygen B-band for monitoring vegetation. *J. Quant. Spectrosc. Radiat. Transf.* 191, 7–12. <https://doi.org/10.1016/j.jqsrt.2017.01.015>.
- Marshak, A., Knyazikhin, Y., Chiu, J.C., Wiscombe, W.J., 2011. Spectrally invariant approximation within atmospheric radiative transfer. *J. Atmos. Sci.* 68, 3094–3111. <https://doi.org/10.1175/JAS-D-11-060.1>.
- Meroni, M., Busetto, L., Colombo, R., Guanter, L., Moreno, J., Verhoef, W., 2010. Performance of spectral fitting methods for vegetation fluorescence quantification. *Remote Sens. Environ.* 114, 363–374. <https://doi.org/10.1016/j.rse.2009.09.010>.
- Mottus, M., Stenberg, P., 2008. A simple parameterization of canopy reflectance using photon recollision probability. *Remote Sens. Environ.* 112, 1545–1551. <https://doi.org/10.1016/j.rse.2007.08.002>.
- Ounis, A., Cerovic, Z.G., Briantais, J.M., Moya, I., 2001. Dual-excitation FLIDAR for the estimation of epidermal UV absorption in leaves and canopies. *Remote Sens. Environ.* 76, 33–48. [https://doi.org/10.1016/S0034-4257\(00\)00190-5](https://doi.org/10.1016/S0034-4257(00)00190-5).
- Pedros, R., Goulas, Y., Jacquemoud, S., Louis, J., Moya, I., 2010. FluorMODleaf: a new leaf fluorescence emission model based on the PROSPECT model. *Remote Sens. Environ.* 114, 155–167. <https://doi.org/10.1016/j.rse.2009.08.019>.
- Porcar-Castell, A., Malenovsky, Z., Magney, T., Van Wittenberghe, S., Fernández-Marín, B., Maignan, F., Zhang, Y., Masey, K., Atherton, J., Albert, L.P., Robson, T. M., Zhao, F., Garcia-Plazaola, J.I., Ensminger, I., Rajewicz, P.A., Grebe, S., Tikkanen, M., Kellner, J.R., Ihalainen, J.A., Rascher, U., Logan, B., 2021. Chlorophyll a fluorescence illuminates a path connecting plant molecular biology to earth-system science. *Nat. Plants*. <https://doi.org/10.1038/s41477-021-00980-4>.
- Rajewicz, P.A., Zhang, C., Atherton, J., Van Wittenberghe, S., Riikonen, A., Magney, T., Fernandez-Marín, B., Plazaola, J.I.G., Porcar-Castell, A., 2023. The photosynthetic response of spectral chlorophyll fluorescence differs across species and light environments in a boreal forest ecosystem. *Agric. For. Meteorol.* 334. <https://doi.org/10.1016/j.agrformet.2023.109434>.
- Rosema, A., Verhoef, W., Schroote, J., Snel, J., 1991. Simulating fluorescence light-canopy interaction in support of laser-induced fluorescence measurements. *Remote Sens. Environ.* 37, 117–130. [https://doi.org/10.1016/0034-4257\(91\)90023-Y](https://doi.org/10.1016/0034-4257(91)90023-Y).
- Smolander, S., Stenberg, P., 2005. Simple parameterizations of the radiation budget of uniform broadleaved and coniferous canopies. *Remote Sens. Environ.* 94, 355–363. <https://doi.org/10.1016/j.rse.2004.10.010>.
- Stenberg, P., 2007. Simple analytical formula for calculating average photon recollision probability in vegetation canopies. *Remote Sens. Environ.* 109, 221–224. <https://doi.org/10.1016/j.rse.2006.12.014>.
- Stenberg, P., Möttus, M., Rautiainen, M., 2016. Photon recollision probability in modelling the radiation regime of canopies — a review. *Remote Sens. Environ.* 183, 98–108. <https://doi.org/10.1016/j.rse.2016.05.013>.
- Sun, Y., Frankenberg, C., Wood, J.D., Schimel, D.S., Jung, M., Guanter, L., Drewry, D.T., Verma, M., Porcar-Castell, A., Griffis, T.J., Gu, L., Magney, T.S., Köhler, P., Evans, B., Yuen, K., 2017. OCO-2 advances photosynthesis observation from space via solar-induced chlorophyll fluorescence. *Science* 358. <https://doi.org/10.1126/science.aam5747>.
- Suñla, P., Nauš, J., 2007. A Monte Carlo study of the chlorophyll fluorescence emission and its effect on the leaf spectral reflectance and transmittance under various conditions. *Photochem. Photobiol. Sci.* 6, 894–902. <https://doi.org/10.1039/b618315h>.
- van der Tol, C., Verhoef, W., Timmermans, J., Verhoef, A., Su, Z., 2009. An integrated model of soil-canopy spectral radiances, photosynthesis, fluorescence, temperature and energy balance. *Biogeosciences* 6, 3109–3129. <https://doi.org/10.5194/bg-6-3109-2009>.
- van der Tol, C., Vilfan, N., Dauwe, D., Cendrero-Mateo, M.P., Yang, P., 2019. The scattering and re-absorption of red and near-infrared chlorophyll fluorescence in the models Fluspect and SCOPE. *Remote Sens. Environ.* 232, 111292. <https://doi.org/10.1016/j.rse.2019.111292>.
- Vilfan, N., van der Tol, C., Müller, O., Rascher, U., Verhoef, W., 2016. Fluspect-B: a model for leaf fluorescence, reflectance and transmittance spectra. *Remote Sens. Environ.* 186, 596–615. <https://doi.org/10.1016/j.rse.2016.09.017>.
- Willmott, C.I., 1981. On the validation of models. *Phys. Geogr. 2* (2), 184–194. <https://doi.org/10.1080/02723646.1981.10642213>.
- Wu, S., Zeng, Y., Hao, D., Liu, Q., Li, J., Chen, X., Asrar, G.R., Yin, G., Wen, J., Yang, B., Zhu, P., Chen, M., 2021. Quantifying leaf optical properties with spectral invariants theory. *Remote Sens. Environ.* 253, 112131. <https://doi.org/10.1016/j.rse.2020.112131>.
- Zeng, Y., Xu, B., Yin, G., Wu, S., Hu, G., Yan, K., Yang, B., Song, W., Li, J., 2018. Spectral invariant provides a practical modeling approach for future biophysical variable estimations. *Remote Sens.* 10, 1508. <https://doi.org/10.3390/rs10101508>.
- Zeng, Y., Badgley, G., Dechant, B., Ryu, Y., Chen, M., Berry, J.A., 2019. A practical approach for estimating the escape ratio of near-infrared solar-induced chlorophyll fluorescence. *Remote Sens. Environ.* 232, 111209. <https://doi.org/10.1016/j.rse.2019.05.028>.
- Zeng, Y., Badgley, G., Chen, M., Li, J., Anderegg, L.D.L., Kornfeld, A., Liu, Q., Xu, B., Yang, B., Yan, K., Berry, J.A., 2020. A radiative transfer model for solar induced fluorescence using spectral invariants theory. *Remote Sens. Environ.* 240, 111678. <https://doi.org/10.1016/j.rse.2020.111678>.
- Zeng, Y., Chen, M., Hao, D., Damm, A., Badgley, G., Rascher, U., Johnson, J.E., Dechant, B., Siegmann, B., Ryu, Y., Qiu, H., Krieger, V., Panigada, C., Celesti, M., Miglietta, F., Yang, X., Berry, J.A., 2022. Combining near-infrared radiance of vegetation and fluorescence spectroscopy to detect effects of abiotic changes and stresses. *Remote Sens. Environ.* 270, 112856. <https://doi.org/10.1016/j.rse.2021.112856>.
- Zhang, Y., Guanter, L., Berry, J.A., van der Tol, C., Yang, X., Tang, J., Zhang, F., 2016. Model-based analysis of the relationship between sun-induced chlorophyll fluorescence and gross primary production for remote sensing applications. *Remote Sens. Environ.* 187, 145–155. <https://doi.org/10.1016/j.rse.2016.10.016>.
- Zhao, F., Ni, Q., 2018. A model to simulate the radiative transfer of fluorescence in a leaf. In: *The International Archives of the Photogrammetry, Remote Sensing and Spatial Information Sciences XLII-3*, pp. 2347–2351. <https://doi.org/10.5194/isprs-archives-XLII-3-2347-2018>.